

Electronic Supplementary Information (ESI) for:

## **A Continuous Flow Chemistry Approach for the Ultrafast and Low-Cost Synthesis of MOF-808**

Sujay Bagi<sup>1,2</sup>, Shuai Yuan<sup>2,3</sup>, Sergio Rojas-Buzo<sup>4</sup>, Yang Shao-Horn<sup>2,3</sup>, Yuriy Román-Leshkov<sup>2\*</sup>

<sup>1</sup> Department of Mechanical Engineering, Massachusetts Institute of Technology, 77 Massachusetts Avenue, Cambridge, Massachusetts 02139, United States.

<sup>2</sup> Department of Chemical Engineering, Massachusetts Institute of Technology, 77 Massachusetts Avenue, Cambridge, Massachusetts 02139, United States.

<sup>3</sup> Department of Materials Science and Engineering, Massachusetts Institute of Technology, 77 Massachusetts Avenue, Cambridge, Massachusetts 02139, United States.

<sup>4</sup> Instituto de Tecnología Química, UPV-CSIC, Universitat Politècnica de València-Consejo Superior de Investigaciones Científicas. Avenida de los Naranjos s/n 46022 Valencia, Spain.

\* Corresponding Author: [yroman@mit.edu](mailto:yroman@mit.edu)

| <b>Table of Contents</b>    | <b>Page</b> |
|-----------------------------|-------------|
| 1. Flow Reactor Platform    | S2 – S4     |
| 2. Materials and Methods    | S4 – S8     |
| 3. Techno-economic Analysis | S9 – S15    |
| Figures S1 – S15            | S16 – S29   |
| Tables S1 – S12             | S30 – S41   |
| References                  | S42 – S43   |

## 1. Flow Reactor Platform

A modular flow synthesis apparatus used in this study was built using components that were available commercially along with a few custom-built critical modules to achieve fast heat transfer, isothermal temperature distribution in the reaction zone, optimal mixing, and fast sampling. Detailed descriptions of liquid handling modules, fluidic connections and the crystallizer apparatus are provided in our previous study.<sup>1-2</sup> Fig. S1 provides a schematic for the setup and calculations for bubble-point pressure to maintain stable reactor operation. Flow synthesis was performed at a minimum pressure of 4 atm for a reaction temperature of 150 °C to avoid the formation of gas bubbles, which have a deleterious effect on the durability of reactor tubing and the MOF crystallization process. The apparatus contains the following key elements: A positive displacement pump (Vici M6 from Valco Instruments) and a syringe pump (PHD Ultra from Harvard apparatus) were used to inject the continuous phase (silicone oil) and the dispersed phase (the precursor mixture), respectively, into a polytetrafluoroethylene (PTFE) T-joint to generate a biphasic slug flow. The reactor tubing (1/8" OD, 1/16" ID) made from PTFE was acquired from Cole-Parmer with an operational temperature up to 260 °C. Length of the tubing used in the heated reaction zone (i.e. the crystallizer unit) was ~8 m. Other fluidic connections such as compression unions and ferrules were made from PTFE and procured from Parker Hannifin. The heated reaction zone was custom built using the following commercially available parts: a sleeve heater furnace from Tempco, three 9 inch long and 1.01 mm wide K-type thermocouples from Omega and a digi-sense programmable temperature controller from Cole-Parmer. The high temperature insulation made from ceramic wool, along with fixtures, clamps and lab jacks to support the crystallizer unit were purchased from McMaster-Carr. High-pressure cylinders of 150 mL capacity with female NPT connections (for sample inflow and pressurizing the chamber) were acquired from Swagelok along with 3-way valves, unions, pressure gauges and other fittings.

Synthesized samples were transferred into 50 mL centrifuge tubes, washed thrice with *N,N*-dimethylformamide (DMF), and acetone. Samples were solvent exchanged with DMF for three days during which DMF was replaced every day. The DMF exchanged MOF-808 was immersed in acetone for three days during which acetone was replaced every day. The solvent-exchanged sample was vacuum dried at 22 °C for 12 h and activated under dynamic vacuum at 120 °C for 24 h before N<sub>2</sub> adsorption measurements.

We reused the silicone oil (Alfa Aesar #A1272822) collected post-synthesis up to three times in subsequent syntheses without seeing any adverse effects on the stability of the biphasic liquid-liquid slug flow or the crystallization process. Silicone oil is both immiscible and inert with respect to the reaction mixture. Post-reaction it can easily be decanted without requiring an additional setup for recovery and purification. We investigated the use of paraffin oil as a continuous phase and observed that it mixed or interacted with the dispersed phase (MOF precursor) during crystallization reactions. This affected both the crystallinity and yield values, thereby making it unsuitable for reactions in flow. The thermal conductivity coefficient for both paraffin and silicone oil is ~0.140 W/(m.K), which is important for fast heat transfer. Hence, silicone oil was chosen as the continuous phase in our reactor.

The use of water as a greener solvent for dissolving H<sub>3</sub>BTC linker was evaluated in our study. However, unlike the DMF solvent, the H<sub>3</sub>BTC linker has poor solubility in water at 20 °C, which generates a ‘slurry-like’ reaction mixture that complicates the operation of the flow reactor in a biphasic slug-flow configuration. We note that all the reagents must be completely soluble in the solvent before injection to ensure reproducibility in the microfluidic flow reactor. This requirement ensures that a homogeneous composition is achieved in every slug to simulate a series of well-mixed micro batch reactors with identical compositions and residence times. Injecting a ‘slurry-

like' reaction mixture results in variation of the relative linker concentration (RLC) and Metal:Linker (M:L) molar ratios in the slugs, thereby affecting both the crystallinity and yield of MOF-808. The use of water is out of scope for the current work due to extensive modifications required for our flow reactor to accommodate 'slurry-like' reaction mixture.

UHP N<sub>2</sub> gas was used to pressurize the system. Table S1 and S2 provide an overview of the flowrates used to obtain specific residence times and physiochemical properties of silicone oil used in flow reactions. A volumetric ratio of 1:2 Oil:Precursor was maintained to maximize the productivity of the process and operate in a stable biphasic flow regime. Higher volumetric ratio of precursor would lead to hydrodynamic failure of the reactor due to large amount of crystals clogging the tubing. Higher volume slugs also results in low mixing efficiency due to stagnation zones developed in larger slugs. A supplementary video file Video S1 captures biphasic slug flow at four different residence times (5, 15, 30 and 120 min); precursor slugs encapsulated by silicone oil (continuous phase) contains MOF-808 nanoparticles exiting the reactor.

## 2. Materials and Methods

All reagents were commercially purchased. They are summarized below: *N,N*-dimethylformamide (99.8%, Millipore), formic acid (purity > 98%), and anhydrous methanol were obtained from EMD Millipore Chemicals. Anhydrous acetone was procured from Acros Organics. Zirconium oxychloride octahydrate (ZrOCl<sub>2</sub>·8H<sub>2</sub>O, purity ≥ 99.5%), and 1,3,5-Benzenetricarboxylic acid (H<sub>3</sub>BTC linker) was obtained from Sigma-Aldrich. Silicone oil (Dimethyl polysiloxane) for flow synthesis with the usable range of -40 °C to 200 °C was procured from Alfa Aesar.

Synthesis of MOF-808 in Batch: Microcrystalline powder samples of MOF-808 were synthesized based on synthetic procedure reported by Jiang et al.<sup>3</sup> H<sub>3</sub>BTC (70 mg, 0.33 mmol) and ZrOCl<sub>2</sub>·8H<sub>2</sub>O (323.3 mg, 1.003 mmol) were dissolved in DMF/formic acid (15 mL/15 mL)

mixture and placed in a 100 mL screw-capped glass jar, which was heated to 130 °C for 48 h. MOF-808 precipitated as white solids that were collected by filtration and washed with DMF, and acetone; the solids were solvent-exchanged and activated as described above.

*Powder X-ray diffraction (PXRD)* patterns were recorded with a Bruker D8 Advance II diffractometer equipped with a  $\theta/2\theta$  Bragg-Brentano geometry and Ni-filtered  $\text{CuK}\alpha$  radiation ( $K\alpha_1 = 1.5406 \text{ \AA}$ ,  $K\alpha_2 = 1.5444 \text{ \AA}$ ,  $K\alpha_2/K\alpha_1 = 0.5$ ). The tube voltage and current were 40 kV and 40 mA, respectively. Samples for PXRD were prepared by placing a thin layer of the appropriate material on a zero-background silicon crystal plate. Fig. S2 (a, b) shows the PXRD patterns for the flow synthesized samples with varied levels of crystallinity along with background correction scheme used for measuring the relative crystallinity.

*Relative Crystallinity (% RC)* measurements were calculated using the HighScore Plus analysis package from Panlytical. During the course of optimization of synthesis parameters, many reaction conditions resulted in a semi-crystalline or an amorphous material. Given that the material crystallinity is an indispensable characteristic, the equation S1 was used to quantify the RC of all synthesized samples. We subtracted the constant background intensity ( $I_{\text{const.bkgd}}$ ) from the total intensity ( $I_{\text{tot}}$ ) to remove substantial contributions to the signal from amorphous phases found in semi-crystalline samples. The intensity contribution from crystalline peaks ( $I_{\text{cryst}}$ ) was calculated using the corrected background, which was computed by an iterative method developed by Sonneveld et al.<sup>4</sup> that takes into account granularity of the background fitting and bending factors pertaining to the curvature.

$$\text{Relative Crystallinity (\% RC)} = 100 \times \left( \frac{\sum I_{\text{cryst.}}}{(\sum I_{\text{total}} - \sum I_{\text{const. bkgd}})} \right) \quad (\text{Equation S1})$$

A summary of the investigated MOF-808 reaction conditions for the rapid optimization of synthesis design space (in flow reactor platform) is provided in Table S3. Calculations for yield and productivity are described in Table S4 and S5. We also used the Caglioti equation to fit the FWHM data points obtained for the peaks in the XRD pattern. The Caglioti equation, described below (Equation S2), establishes a relationship between broadening (B) and the fitting parameters W, V, and U that are derived as an instrument response function for X-ray diffraction. The curve fit provides Lorentz and Gauss coefficients that account for crystal shape factor K and instrument broadening.

Caglioti equation:

$$B^2 = (W + V \tan \theta + U \tan^2 \theta) \quad (\text{Equation S2})$$

*Scanning Electron Microscopy (SEM)* images were acquired using Zeiss Merlin High-resolution SEM. Double coated conductive carbon tape was glued to an aluminum sample mount (or stubs, 12.7 mm diameter) to minimize charging of non-conductive MOF sample and acquire high-resolution images. Small amount of sample was transferred to the mount using a spatula and excess sample was dusted off using compressed air blown for a few seconds. Sample mounts were then sputter coated with an ultra-thin layer (~10 nm) of Au/Pd (Gold and Platinum electrode), to improve resolution of edge features on the sample, reduce charging and acquire high quality images of poorly conducting samples. The SEM operational parameters such as working distance, probe current and acceleration voltage are listed below every image acquired. Fig. S3 shows SEM images comparing batch and flow synthesized samples.

*Transmission Electron Microscopy (TEM)* images were acquired using FEI Tecnai Multipurpose Digital TEM. MOF sample was added to a glass vial containing acetone and shaken to obtain a

well-dispersed suspension. A drop or two of this suspension was added to the copper grid (5-6 nm thick and 3.05 mm wide) with a thin film of pure carbon deposited on one side (CF200-CU from Electron Microscopy Sciences). After the evaporation of acetone, the grid was placed on the sample holder and inserted in the beam column. The chamber was evacuated at  $3.2\text{E-}7$  torr before the electron gun was switched on and aligned for acquiring high-resolution images. The TEM was operated at 120 kV and corrected for image aberrations using stigmator in condenser/objective lens. Fig. S4 shows a comparison of TEM images acquired for MOF samples in batch and flow syntheses, while Fig. S5 compares morphology of isolated crystals obtained in flow and corresponding SAED pattern. Fig. S6 compares average size distribution of nanoparticles measured using SEM and TEM micrographs. Microcrystalline MOF-808 samples synthesized from batch and flow syntheses were imaged using a high resolution transmission electron microscope (TEM) and the corresponding crystal sizes were measured using the ImageJ software program based on a procedure reported by Hirschle et al.<sup>5</sup>

*Nitrogen adsorption and desorption isotherms* were measured by using a Quantachrome Autosorb iQ apparatus at liquid nitrogen temperature (77 K). A typical sample mass of ca. 50 mg of MOF-808 was pre-activated at 120 °C for 24 h to remove all residual solvent, before measurement. Free space correction measurements were performed using ultra-high purity He gas (UHP grade 5, 99.999% pure). Oil-free vacuum pumps were used to prevent contamination of sample or feed gases. Fig. S8 plots the linear region of the BET equation ( $0.05 < P_0 < 0.15$ ) which satisfies the first consistency criterion of the BET theory.<sup>6</sup> The data points in this region had a  $R^2 > 0.997$  obtained from linear regression.

*Thermogravimetric Analysis (TGA)* was performed in air environment with a heating rate of 5 °C.min<sup>-1</sup> on TQA 500 of TA Instruments. Fig. S9 provides TGA trace and derivative weight loss

curves for samples synthesized in batch and flow. Table S11 compares the percentage defects in MOF-808 samples synthesized in flow and batch reactors using a procedure reported in previous studies.<sup>7-8</sup>

### 3. Techno-economic Analysis (TEA)

A process-based cost estimation methodology was employed to assess production costs, which mimics the actual steps of synthesis (from raw materials to finished product) and determines the final cost by summing individual costs incurred in each of the steps.<sup>9</sup> In order to streamline the techno-economic analysis (TEA), we only consider production costs directly related to the MOF synthesis and ignore indirect costs and labor costs. The system boundary for the TEA showing inputs and outputs to the model along with a simplified block diagram showing flow of materials, energy consumption, and process waste generated for each unit operation is presented in Fig. S10. A typical lab-scale synthesis starts with dissolving reagents such as metal salt and linker in organic solvents to form the reaction mixture, which is then heated to crystallize MOF particles. The post-processing of the mixture is comprised of separating crystalline solids from the mother liquor via centrifugation, followed by multiple solvent-exchanges and activation of MOF by heating under vacuum. All steps for batch and flow syntheses remain the same except the crystallization process owing to differences in the equipment used. Process waste in the form of used solvent (*N,N*-DMF, and acetone) is generated during centrifugation and activation of the MOF; while solvent recovery and recycling is crucial for a low-cost and sustainable industrial-scale synthesis, it is not practical to implement solvent recycling for a lab-scale operation due to higher capital costs involved for setting up additional infrastructure and uncertainties in solvent purity after recycling.<sup>10-11</sup> The cost associated for executing each unit operation (e.g. crystallization, separation etc.) are added to generate the total cost of synthesis in \$/g for flow and batch syntheses (Equation S3). Material cost reflects the cost of raw materials (metal salt, linker, modulator, and solvents) used in the synthesis, while manufacturing costs reflect the cost of machinery amortized over equipment lifetime as well as process energy, utility costs, and routine maintenance. For a laboratory-scale synthesis, we purchased small quantities of reagents and the price quotes for each of them along with the details

on the equipment used in the lab are described in Tables S6, and S7. For an industrial scale manufacturing of MOFs, bulk purchase of reagents would be required which would result in lower cost of reagents; the inputs for the TEA model can be updated to reflect the purchase prices accordingly. We model two production scenarios to quantify cost and energy associated with lab-scale flow and batch syntheses (Fig. S11); Scenario 1: One time synthesis – represents a typical laboratory operation where MOF is manufactured intermittently in small quantities ca. hundreds of mg scale, which is used for characterization and exploratory work, and Scenario 2: Continuous Production – representing a manufacturing environment where equipment is run continuously to achieve maximum production rates. For a meaningful comparison between the synthetic routes, we match the amount of MOF synthesized for the two processes in Scenario 1, while Scenario 2 evaluates the processes based on the same production rates on a 24 h basis. In case of flow synthesis, we choose a residence time of 5 min for modelling the TEA to compare with the batch synthesis as the baseline. Operational time calculations for batch and flow processes are determined from mass and energy balances for the unit operations which take into account product yield and cycle times (Table S8).

Cost trends for manufacturing MOF-808 in flow and batch syntheses under two scenarios are shown in Fig. S12a Equipment costs dominate the total cost of synthesis for both batch and flow routes in Scenario 1 while materials cost dominate the total cost for both synthetic routes in Scenario 2. Switching from an intermittent to a continuous production resembling an industrial-scale operation lowers the total synthesis cost of MOF-808 to \$11.3/g in batch and \$3/g in flow, representing an expected reduction by ~85% and ~60% respectively. The total cost of synthesis reflects the minimum cost for MOF-808 production under a typical lab-scale environment. Materials cost breakdown shown in Fig. S12b highlights the cost of reagents used for synthesis

and post-process. Lower cost of materials in flow synthesis results from the use of concentrated precursor mixtures that yield higher amount of crystalline solids on a volumetric basis of reaction mixture compared to batch. The costs originating from process solvents (DMF and acetone) that are used in post-process for separation and activation remain the same for both synthetic routes. Costs pertaining to the use of DMF and formic acid dominate the materials cost for both synthetic routes. Flow synthesis sees a dramatic reduction in the use of DMF by ~84% and formic acid by ~67% on a volumetric basis of the reaction mixture compared to batch, resulting in lower costs and a greener process, highlighting the direct benefits of using a concentrated reaction mixture. Fig. S13 shows projections for cost savings achieved in flow by reduction in the use of DMF and formic acid as a function of MOF production on a tens of kg scale. In view of mass production, we consider bulk purchase prices for reagents (Table S7); these projections are achieved by extrapolating the lab-scale cost structure with a goal to quantify costs incurred in batch and flow synthesis and do not consider parameters associated with scaling-up the production such as equipment, storage space etc. Further cost reductions are possible by modifying the unit operations that can minimize the use of expensive solvents or recycling them to achieve a greener synthetic route. Given the excellent hydrothermal stability of MOF-808, modifications in the post-process by replacing the use DMF and acetone with water for solvent-exchange before activation, considerably reduces the cost and process waste generated.<sup>12</sup> Using a relatively cheaper modulator such as acetic acid instead of formic acid reduces materials cost, however it could affect the pore size distribution and surface area of the solids.<sup>13-14</sup> Tradeoffs associated with cost reduction measures related to changes in the equipment, unit operations, and precursor composition should be judiciously considered to balance the product attributes such as surface area, crystallinity with optimal cost of synthesis.

The energy intensity of the process in terms of electrical energy consumed to synthesize a gram of MOF ( $kWh\ g^{-1}$ ) is plotted in Fig. S14, which accounts for the total electricity consumption in all unit operations, along with the corresponding process emissions ( $kgCO_{2-eq}\ g^{-1}$ ). Since electricity is the only form of energy input required for the synthesis, process emissions originate only from the electricity grid and vary linearly as a function of energy consumed in the process. Carbon intensity of the ISO-NE electricity grid in the form of annual average GHG (greenhouse gas) emissions per kWh generated was reported to be  $310\ g\ kWh^{-1}$  in 2017.<sup>15</sup> A detailed breakdown of energy consumed in the equipment is provided in Table S8. Energy intensity of the flow synthesis compared to batch is lower by two orders of magnitude in scenario 1 and an order of magnitude lower in scenario 2, demonstrating significant improvements in energy efficiency achieved in flow. A primary reason for low energy intensity stems from the use of a compact heater in flow synthesis to efficiently heat the miniaturized reaction system with high SA/V ratio that results in a higher productivity, shorter residence time and minimal heat loss, unlike batch synthesis which typically uses convection ovens or heating mantles in a lab-scale environment.<sup>16-</sup>

<sup>18</sup> Moreover, tuning the reaction parameters to avoid the use of harsh solvothermal conditions such as high temperature and pressure will reduce capital and operating expenses.<sup>19-20</sup> Given the wide range of electricity prices (0.07 – 0.29 \$/kWh) across the US,<sup>21</sup> lower electricity prices would further reduce the cost of synthesis. We performed a sensitivity analysis to evaluate the influence of electricity cost on the total cost of synthesis (Fig. S15). A variation of  $\pm 70\%$  of electricity cost from a base value of \$0.12/kWh resulted in  $\pm 9\%$  and  $\pm 2\%$  variation in the total cost of batch and flow synthesis for scenario 1. In case of scenario 2, we see  $\pm 0.5\%$  variation for both synthetic routes; owing to lower energy intensity achieved in flow, energy cost are relatively a small fraction of the total cost. The purpose of this TEA is to identify general trends in batch and flow processes,

costs drivers, mass and energy balances, and potential pathways to curtail the synthesis costs via lower use of solvents and modification in reaction parameters. Given the large number of functional MOFs reported in the literature, a critical assessment and optimization of manufacturing routes in a lab-scale environment serves as a prerequisite for sustainable industrial-scale synthesis paving the way for advent of low cost MOFs in commercial technologies.

Silicone oil used in flow synthesis does not mix with the precursor mixture and is not considered in the materials cost matrix as it can be fully recovered and re-used without additional equipment. Electricity is the only form of energy input required for the synthesis. Average utility costs in the US were \$0.105 per kWh, however commercial utility cost for the state of Massachusetts was \$0.12 per kWh, which is considered for calculations based on price estimates from ISO-NE (Independent System Operator-New England).<sup>15</sup> About 51% of energy mix for the grid came from non-fossil fuel sources including nuclear (31%), while natural gas accounted for 48% of the fossil fuel source of the energy mix.<sup>22</sup> Standard labor rates could vary based on manufacturing environment, however average costs for operator would be ~\$20/person/h and a supervisory person would cost ~\$35/person/h based on estimates from US bureau of labor statistics.<sup>23</sup> Equipment lifetime for all machinery used in the production process, the maintenance costs and consumables are obtained after consultation with corresponding OEMs (Original Equipment Manufacturers) and described in Table S6. Cost incurred for maintenance and consumables on most equipment over its useful life are in a range of ~15-25% of the purchase price. Equations S3–S9 described below are considered for cost and energy accounting in the TEA model and are computed separately for flow and batch syntheses owing to differences in process yield, cycle times, and equipment used for crystallization. Definitions for all parameters used is provided in Table S9. For Scenario 2 as illustrated in Fig. S11, the maximum precursor throughput in the flow

reactor (1/16 inch ID) and a corresponding yield of ~80% leads to a production rate of ca. 33 g of MOF-808 in 24 h. The batch synthesis based on the recipe by Jiang et al.<sup>3</sup> uses a 1000 mL glass jar – is scaled-up to match the production rate achieved in flow. Deviating from using 5 x 1000 mL glass jars to accommodate the precursor mixture to a single 5000 mL glass jar could result in diminished yields and a variation in induction time – MOF synthesis relies on nucleation at reactor vessel surface and changes in surface area to volume (SA/V) ratio of the vessel leads to inconsistencies.<sup>24</sup> Increasing the vessel sizes for batch synthesis also result in large gradients in heat and mass transfer limitations that affect MOF crystallinity and require re-optimization of the process parameters (temperature, induction time) and possibly modifying the heating methods.<sup>25</sup> Forced convection oven used in the study was Yamato DKN-402C with a capacity of 90 L and could easily hold upto 7 glass jars of 1000 mL used in scenario 2. Bulk commodity prices used in Fig. S13 represent the cheapest option, but storage space and additional capital expenditure on infrastructure for handling large volumes of reagents would be required to achieve ca. tens of kg production output.

$$\text{Total Cost of Synthesis } (\$.g^{-1}) = \left( \left( \frac{C_{\text{materials}} + C_{\text{energy}}}{\text{g of MOF-808 synthesized}} \right) + \left( \frac{C_{\text{operation}}}{P_{\text{MOF-808}}} \right) \right) \quad (\text{Equation S3})$$

$$\text{Operational Cost } (\$.day^{-1}) = \sum_{\text{All unit operations}} \left( \frac{n_{\text{machine}} \times C_{\text{machine}} \times C_{\text{Mnt. \& Cons.}}}{t_{\text{life-time}}} \right) \quad (\text{Equation S4})$$

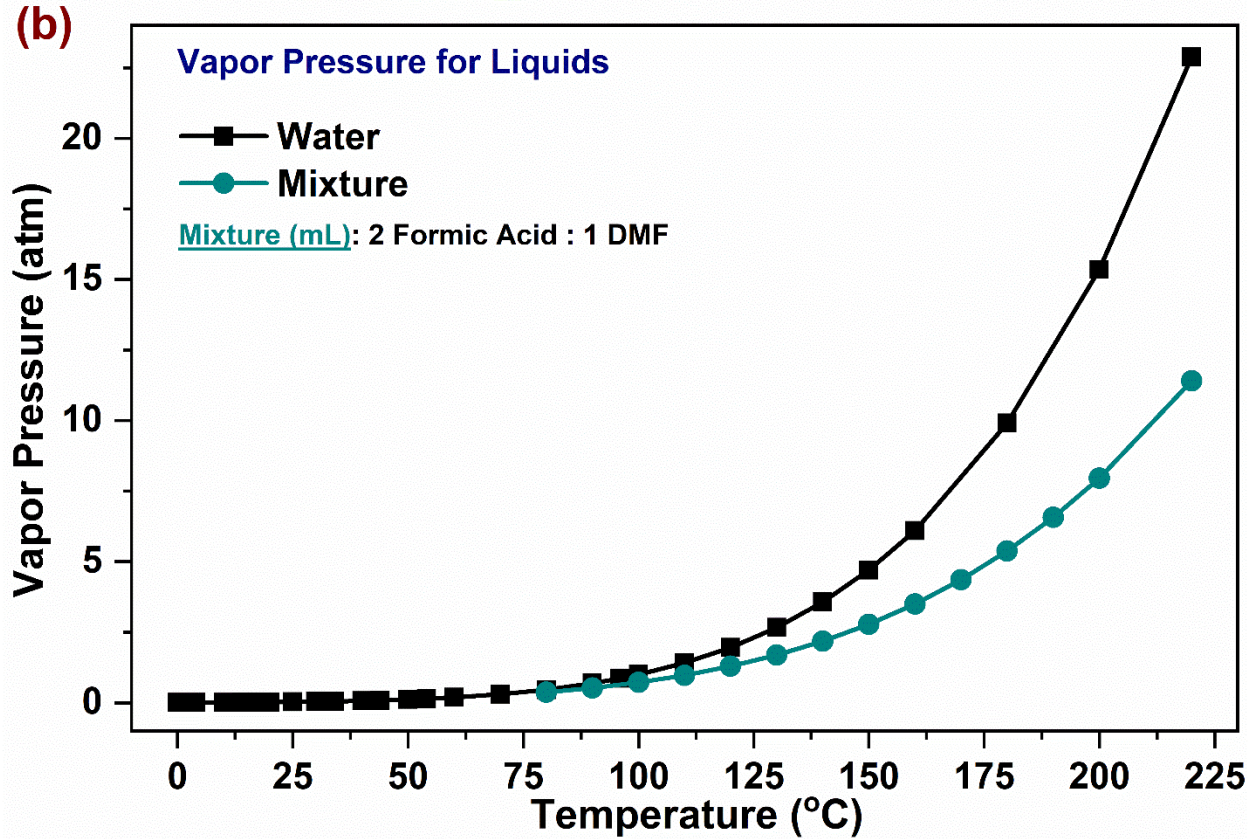
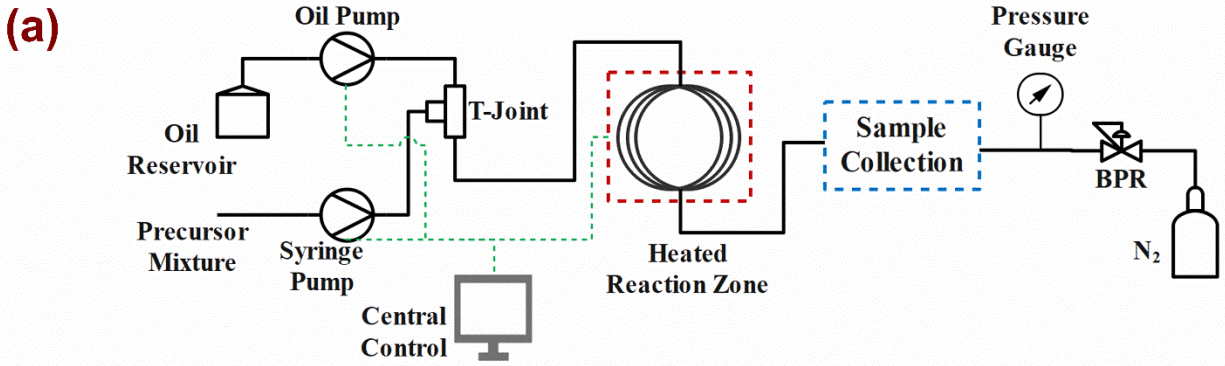
$$\text{Materials Cost of Synthesis } (\$.g^{-1}) = \sum_{\text{All unit operations}} \left( \frac{C_{\text{Zr}} + C_{\text{linker}} + C_{\text{modulator}} + C_{\text{solvents}}}{\text{g of MOF-808 synthesized}} \right) \quad (\text{Equation S5})$$

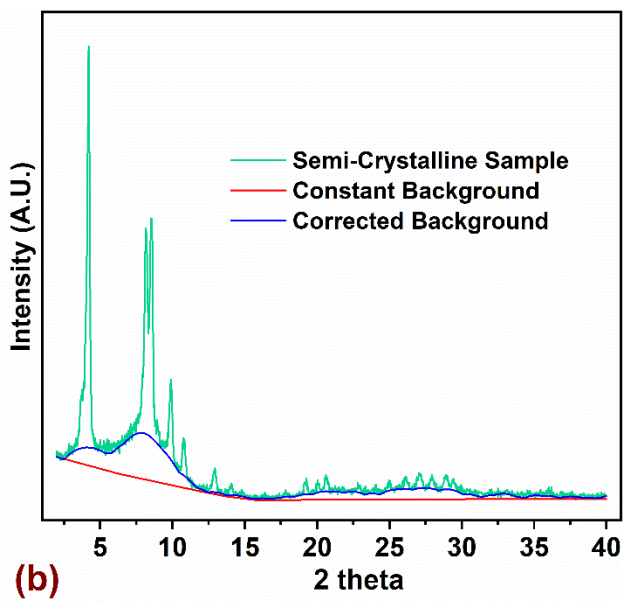
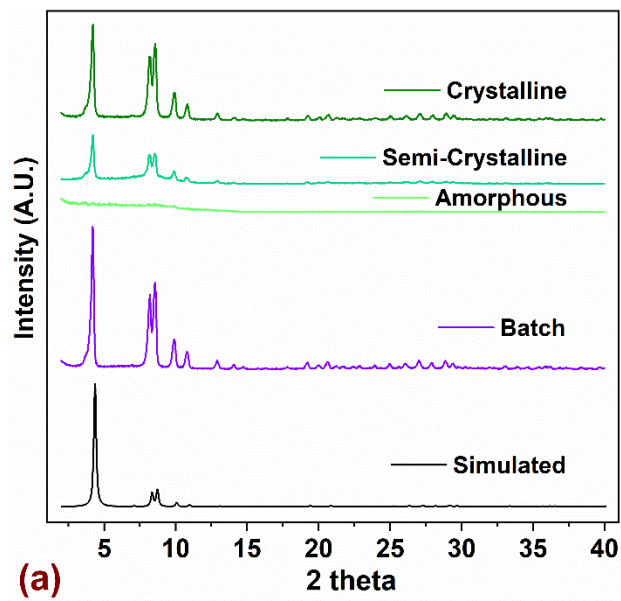
$$\text{Total Energy Cost (\$)} = \sum_{\text{All unit operations}} (E_{\text{machine}} \times C_{\text{electricity}}) \quad (\text{Equation S6})$$

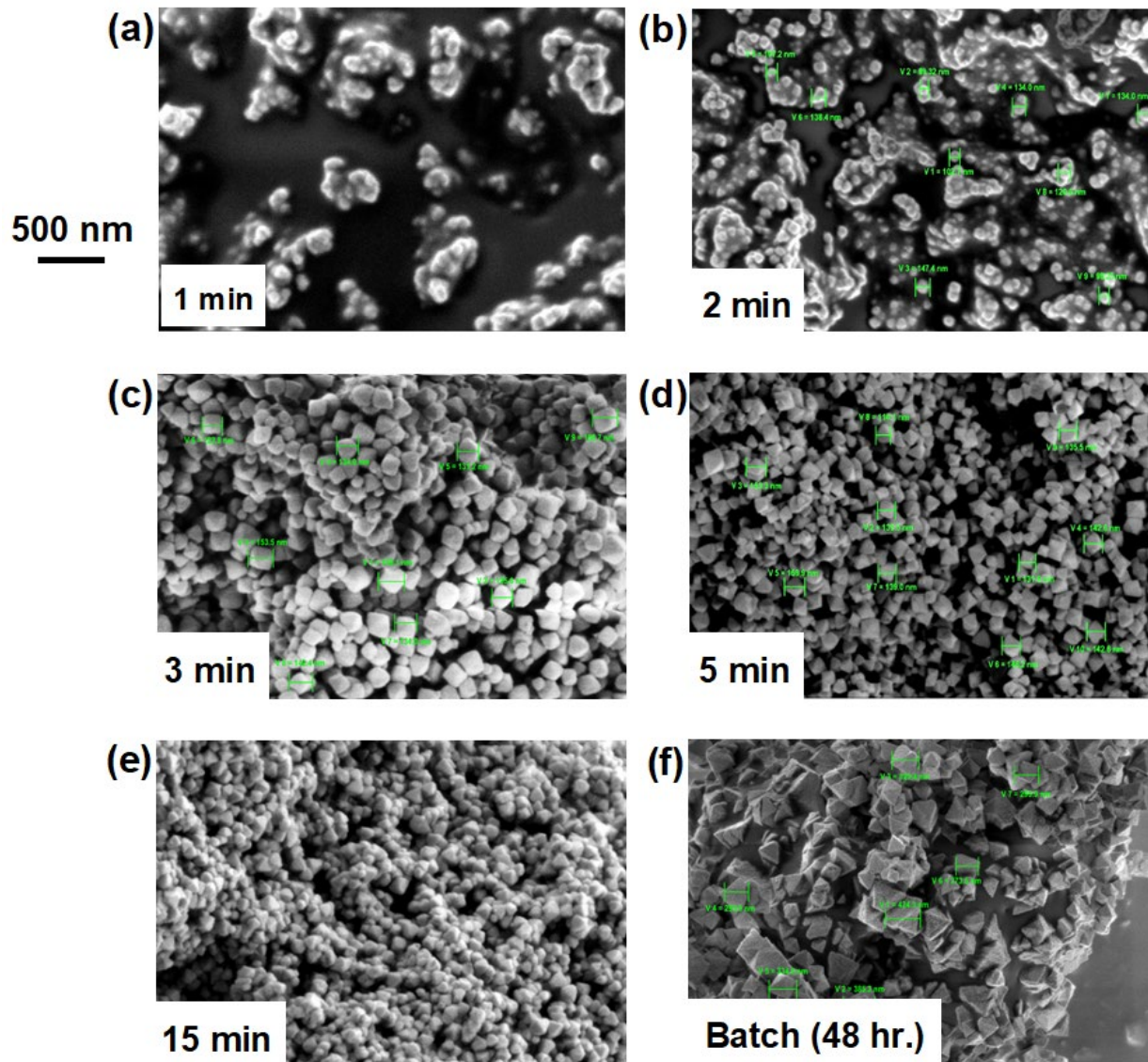
$$\text{Total Equipment Cost (\$)} = \sum_{\text{All unit operations}} (n_{\text{machine}} \times C_{\text{machine}} \times C_{\text{Mnt. \& Cons.}}) \quad (\text{Equation S7})$$

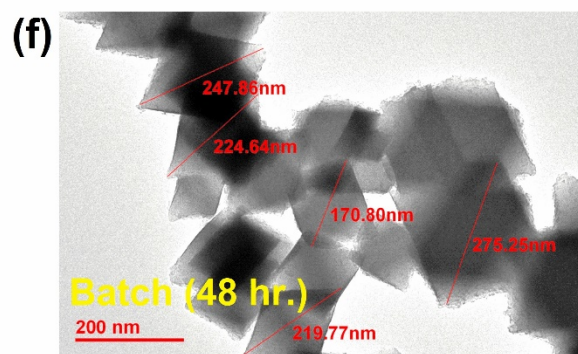
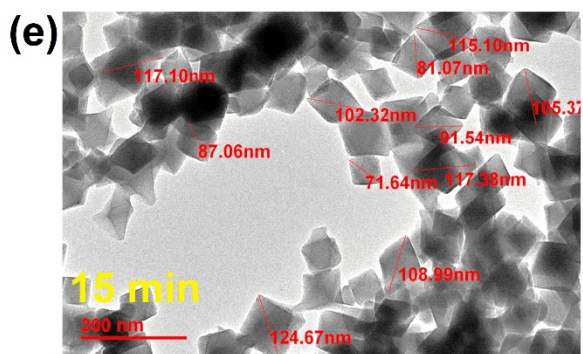
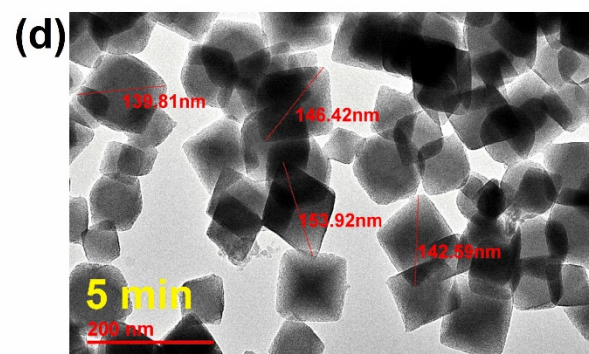
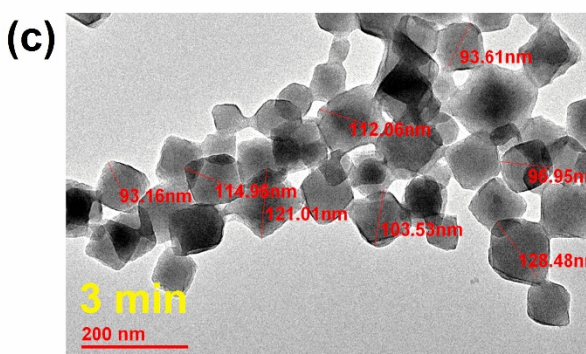
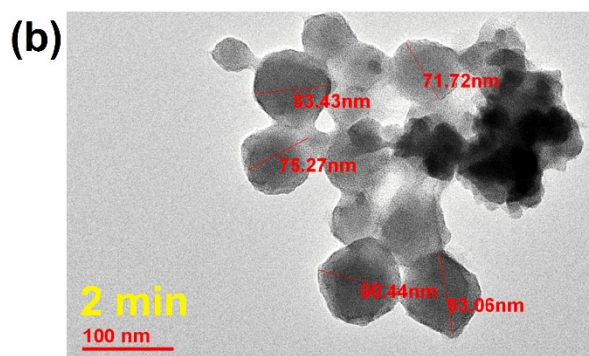
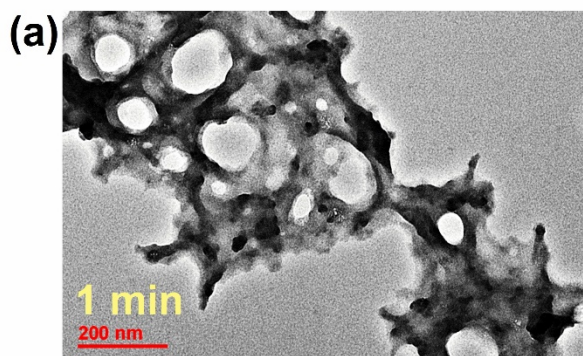
$$\text{Process Energy Intensity (kWh} \cdot \text{g}^{-1}\text{)} = \sum_{\text{All unit operations}} \left( \frac{E_{\text{machine}}}{\text{g of MOF-808 synthesized}} \right) \quad (\text{Equation S8})$$

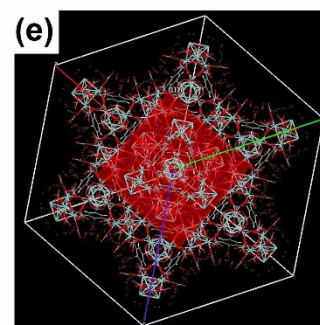
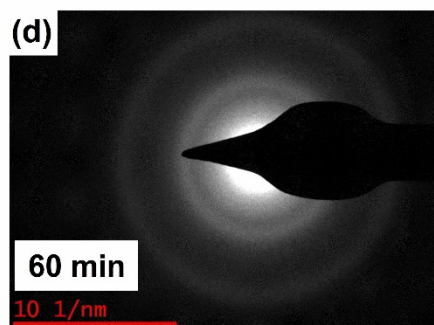
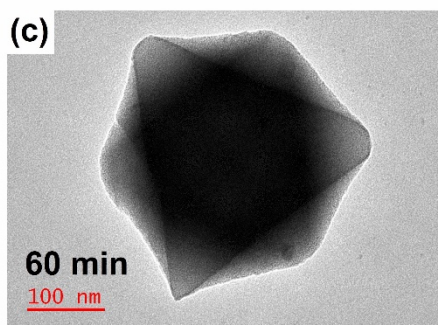
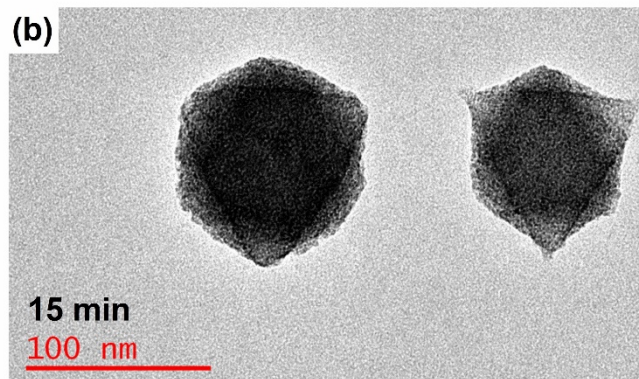
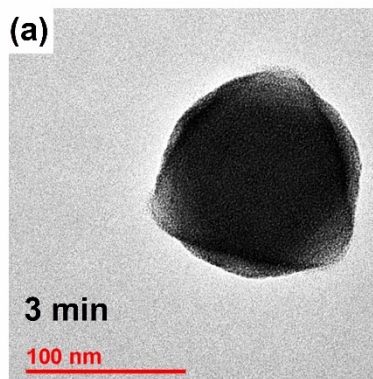
$$\text{Process Emissions (kgCO}_{2\text{-eq}} \cdot \text{g}^{-1}\text{)} = (E_{\text{process}} \times \text{GHG}_{\text{grid}}) \quad (\text{Equation S9})$$

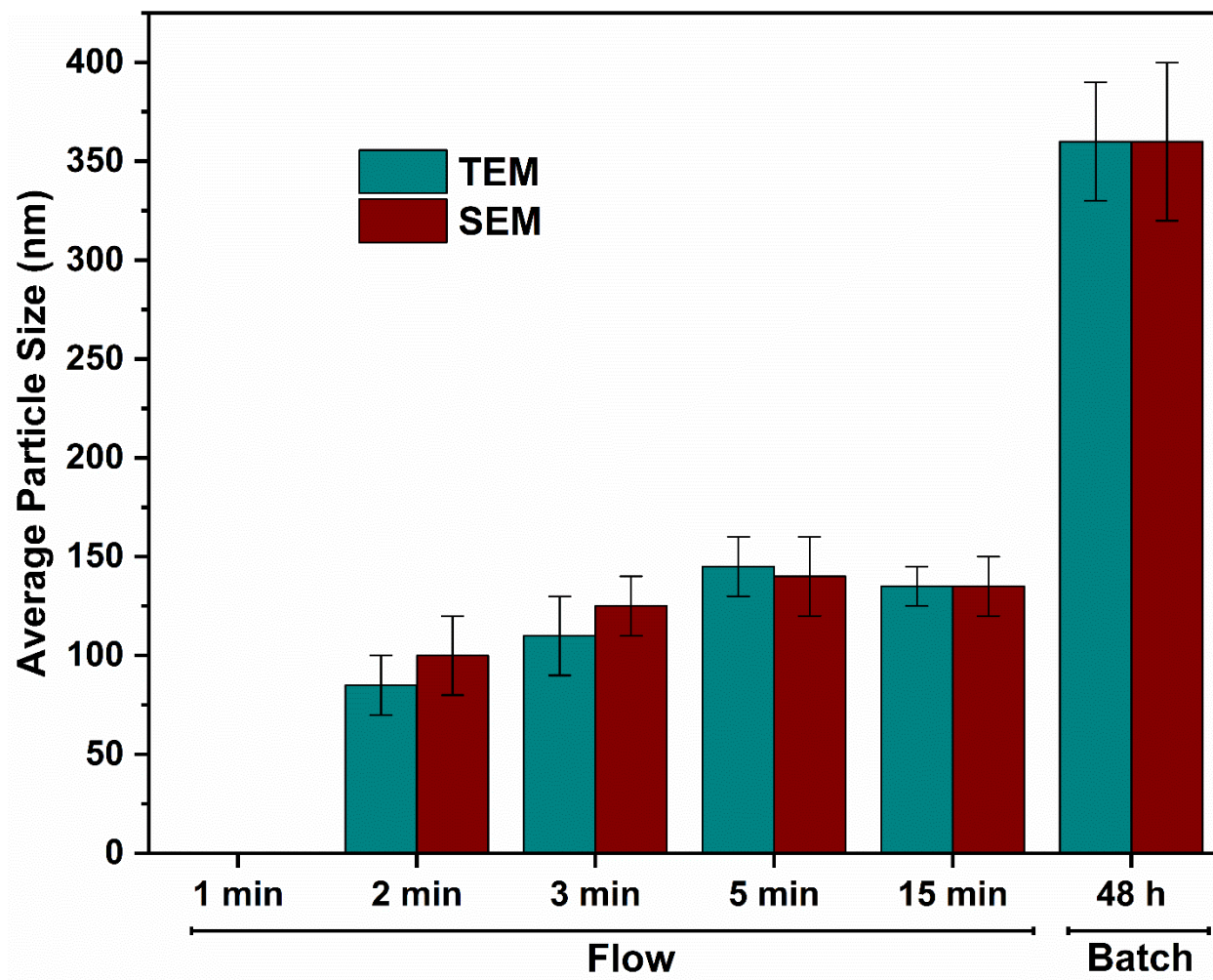


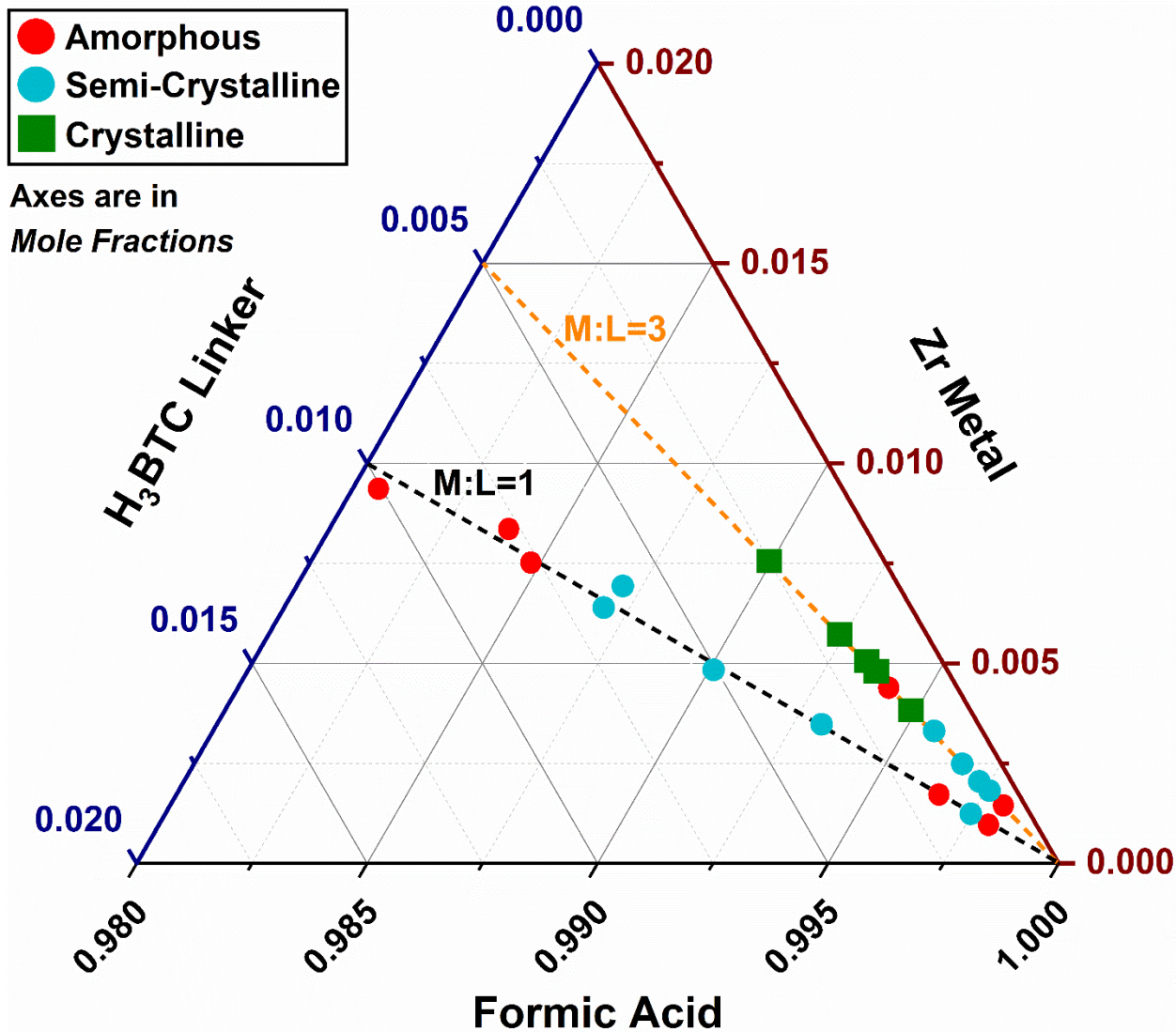


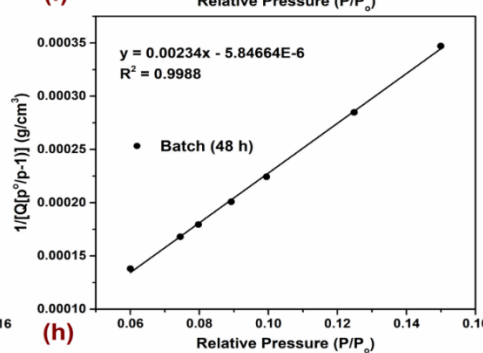
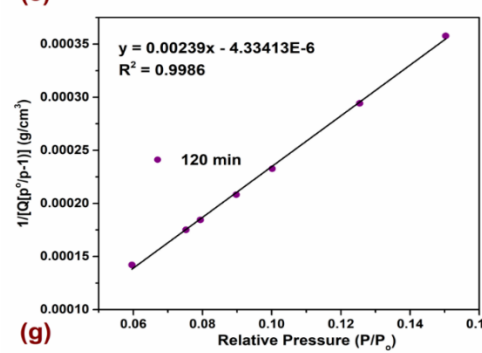
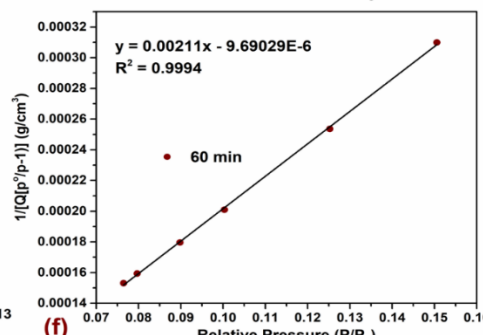
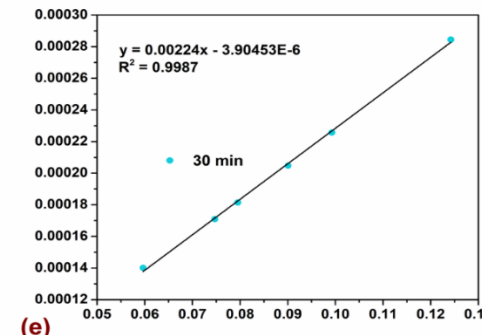
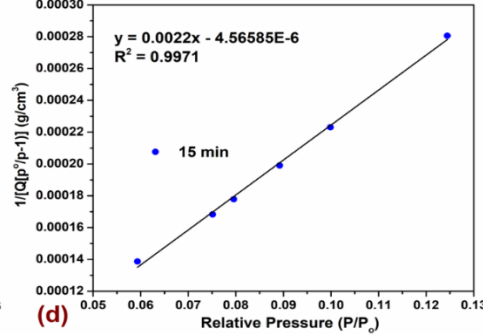
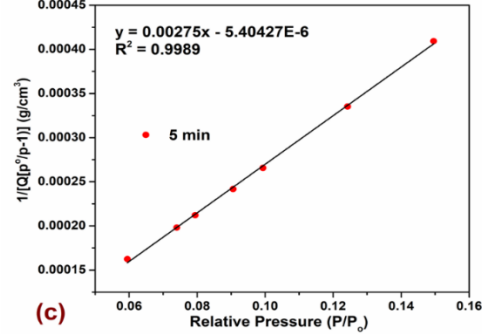
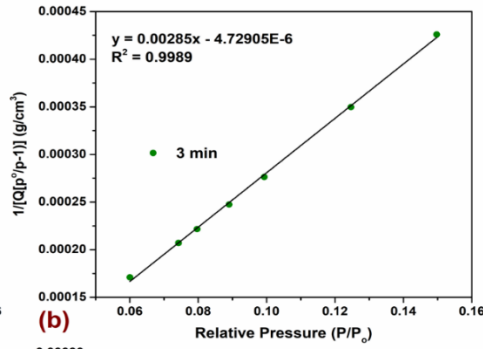
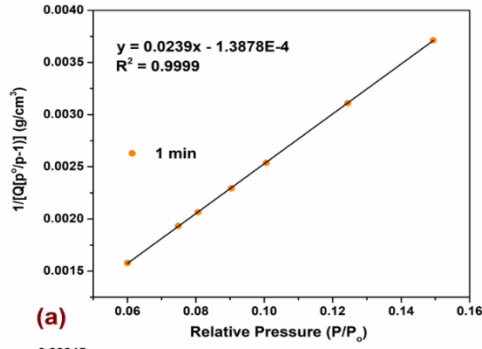






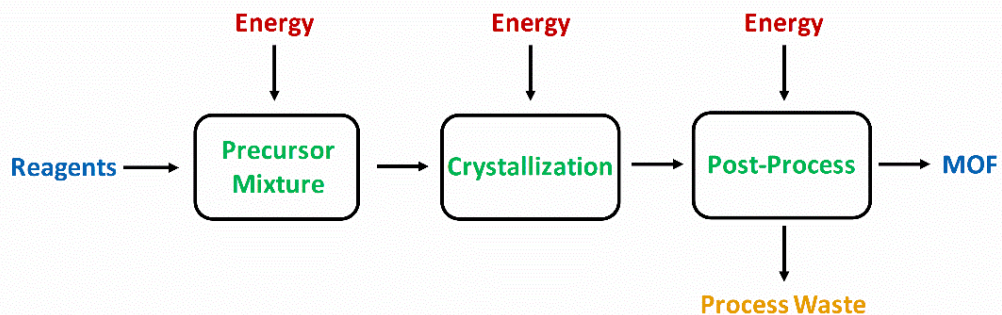






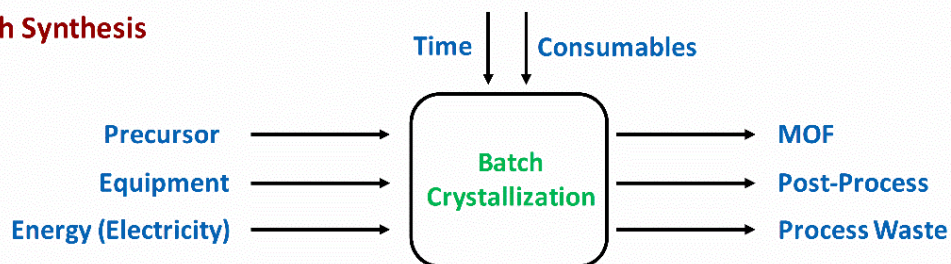


(a)

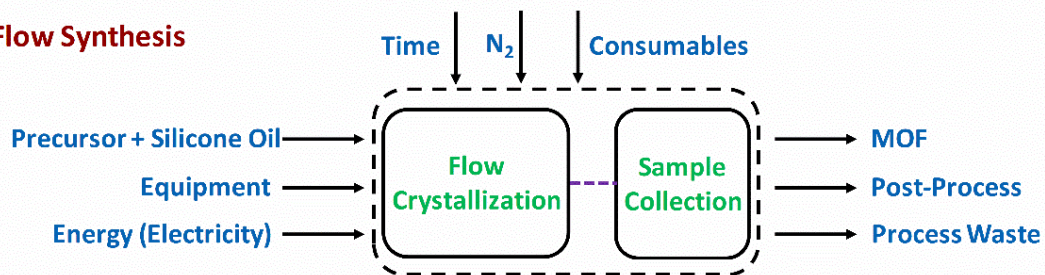


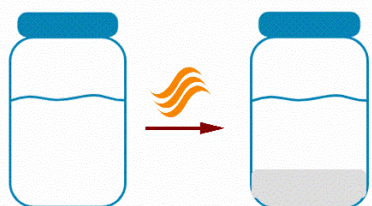
(b)

**Batch Synthesis**



**Flow Synthesis**



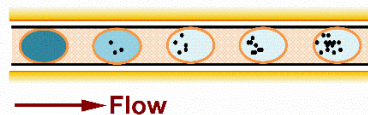


**Scenario 1: One Time Syn. (Intermittent)**  
**Scenario 2: Continuous Production**

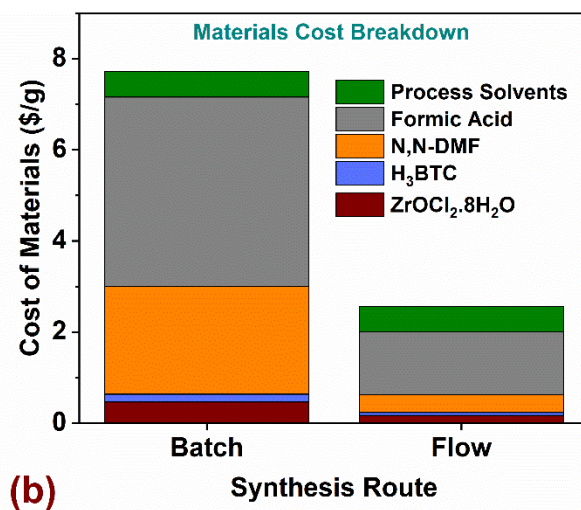
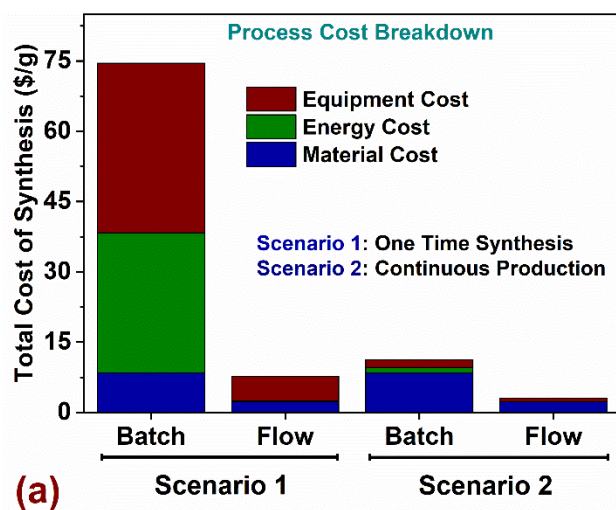
|                   |                        |
|-------------------|------------------------|
| <b>Scenario 1</b> | <b>Scenario 2</b>      |
| 100 mL Glass Jar  | 5 x 1000 mL Glass Jars |
| 0.22 g in 48 h    | 33 g in 24 h           |

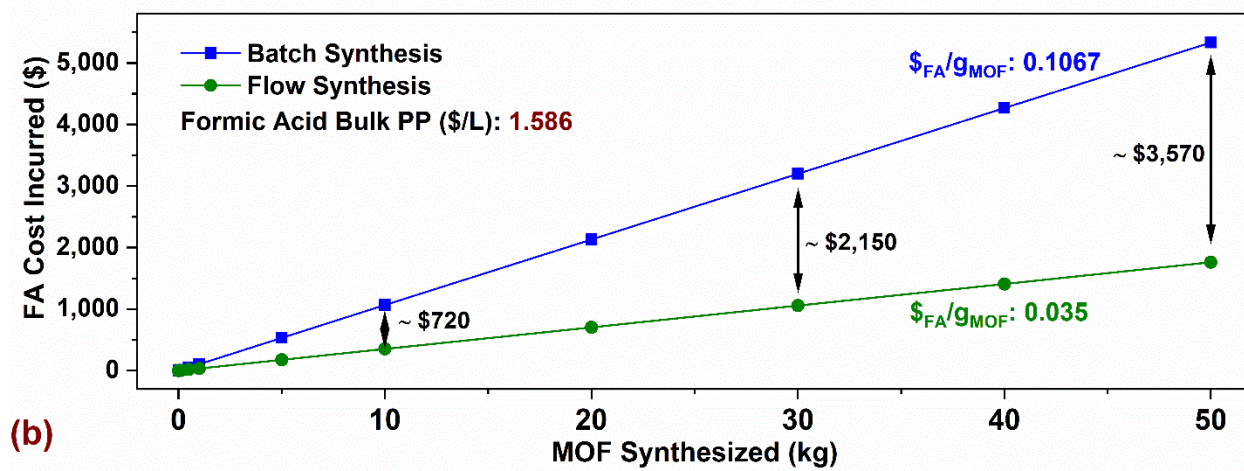
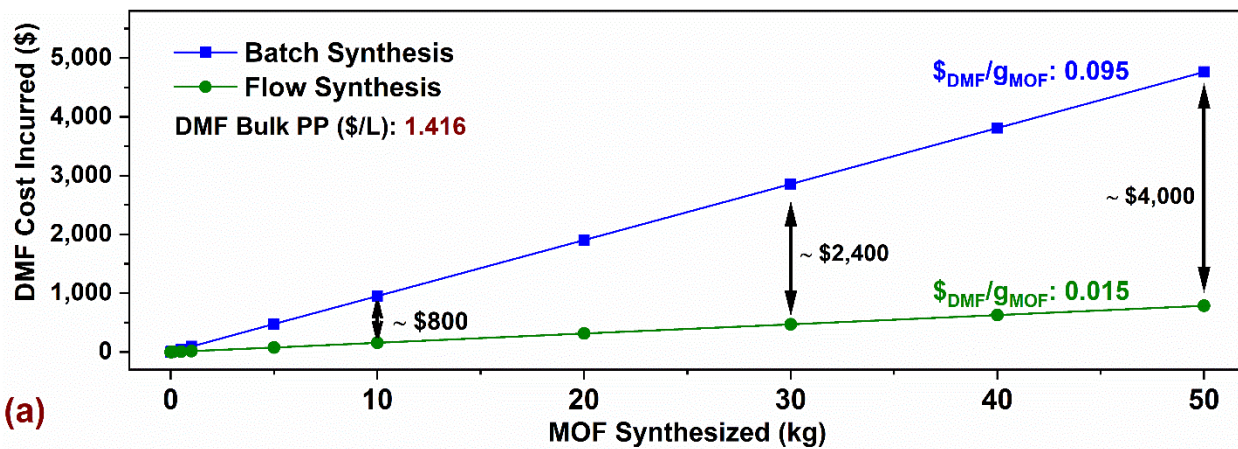
**Batch Synthesis**

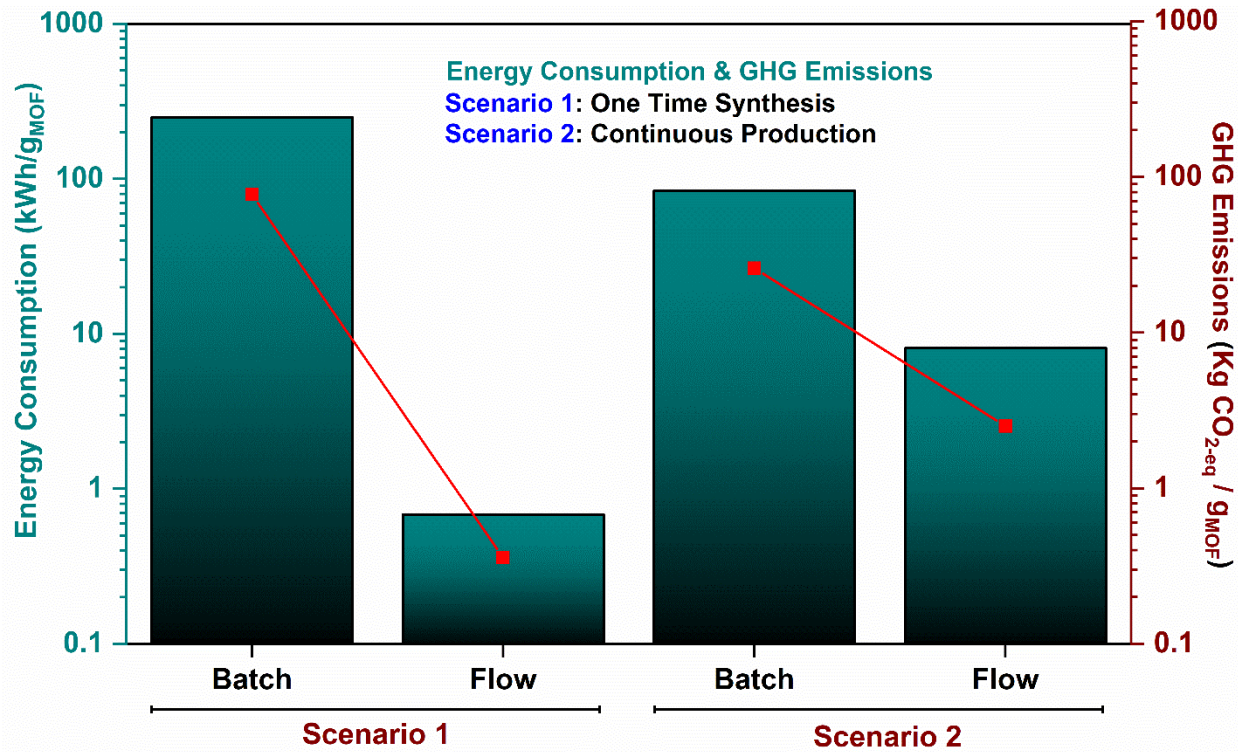
**Flow Synthesis**



|                    |                    |
|--------------------|--------------------|
| <b>Scenario 1</b>  | <b>Scenario 2</b>  |
| 16 mL Reactor Vol. | 16 mL Reactor Vol. |
| 0.22 g in 0.16 h   | 33 g in 24 h       |







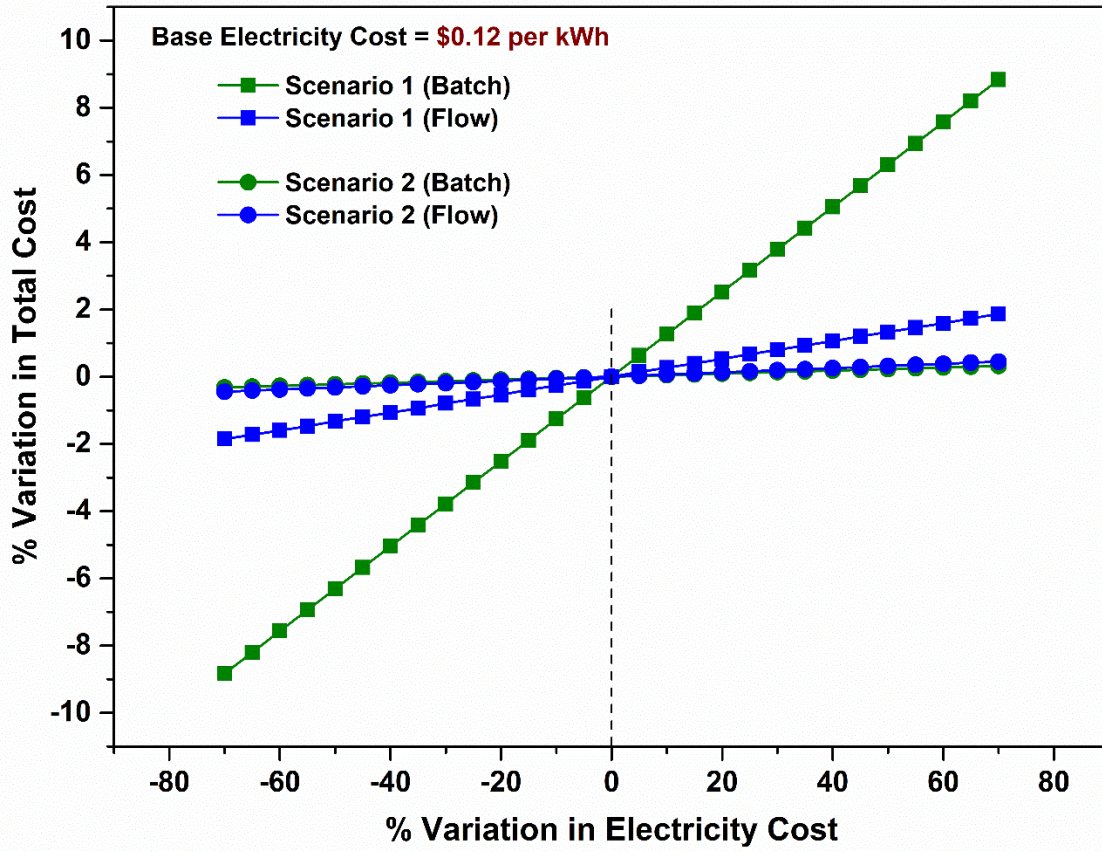


**Table S1.** Residence time for multiple flow rates in a reactor volume of 16 mL. The reactor tubing had an inner diameter of 1/16 in (0.159 cm) with a heated reaction zone length of 8 m.

| Total Flow Rate* (mL/min) |                     |           | Residence Time |              | Linear Velocity |
|---------------------------|---------------------|-----------|----------------|--------------|-----------------|
| Total                     | Oil:Precursor (1:2) |           | min            | hour         | cm/min          |
|                           | Oil                 | Precursor |                |              |                 |
| 16.000                    | 4.8                 | 11.2      | <b>1</b>       | <b>0.016</b> | 808.489         |
| 8.000                     | 2.4                 | 5.6       | <b>2</b>       | <b>0.033</b> | 404.244         |
| 5.333                     | 1.767               | 3.553     | <b>3</b>       | <b>0.05</b>  | 269.36          |
| 3.200                     | 0.96                | 2.24      | <b>5</b>       | <b>0.083</b> | 161.697         |
| 1.600                     | 0.48                | 1.12      | <b>10</b>      | <b>0.166</b> | 80.849          |
| 1.067                     | 0.320               | 0.747     | <b>15</b>      | <b>0.25</b>  | 53.870          |
| 0.534                     | 0.160               | 0.374     | <b>30</b>      | <b>0.50</b>  | 26.900          |
| 0.267                     | 0.080               | 0.187     | <b>60</b>      | <b>1.00</b>  | 13.460          |
| 0.134                     | 0.040               | 0.094     | <b>120</b>     | <b>2.00</b>  | 6.730           |

**Table S2.** Physicochemical properties of silicone oil (continuous phase) and dimensions of tubing used in the reactor for crystallization of MOF-808.

|   |                           |
|---|---------------------------|
| Density of Oil (@ 25°C)                         | 956 kg/m <sup>3</sup>     |
| Kinematic Viscosity Of Oil (@ 25°C)             | 1.2E-05 m <sup>2</sup> /s |
| PTFE Tubing (max operating range)               | 25 atm, 260 °C            |
| T-joint (max operating range)                   | 15 atm, 130 °C            |
| PTFE Tubing Dimensions (in Reactor)             | 1/8" OD, 1/16" ID         |
| Specific Heat Capacity (C <sub>p</sub> ) of Oil | 2000 J/Kg/K               |
| Thermal Conductivity (k) of Oil                 | 0.135 W/m/K               |

**Table S3.** Summary of MOF-808 reaction conditions investigated for rapid optimization of synthesis space using the flow reactor platform at 150 °C. ‘FA:DMF’ denotes the volumetric ratio of Formic Acid to DMF used in the precursor mixture. Every reaction mixture was prepared in a fixed volume of 30 mL where volumetric ratio of FA:DMF was varied. ‘M:L’ represents molar ratio of Zr metal (in the form of  $ZrOCl_2 \cdot 8H_2O$ ) and  $H_3BTC$  linker (benzene-1,3,5-tricarboxylic acid, also known as Trimesic Acid). Linker concentration is varied only in precursor mixtures with M:L = 3, to probe the influence of concentrated precursor on MOF-808 crystallinity. Relative linker concentration (RLC) of 1 corresponds to 70 mg of  $H_3BTC$  in a 30 mL reaction mixture. Higher the concentration of precursor, lower is the ‘FA:M’ molar ratio, which represents moles of Formic Acid to Zr metal in the precursor mixture. Run # 39 was the composition reported by Jiang et al.<sup>3</sup> to synthesize MOF-808 in batch, and was used as a starting composition for optimizing flow synthesis.

| Run # | FA:DMF<br>(Vol. Ratio) | M:L<br>(Molar Ratio) | Relative<br>Linker<br>Concentration | FA:M<br>(Molar Ratio) | Res. Time<br>(min) | %<br>RC |
|-------|------------------------|----------------------|-------------------------------------|-----------------------|--------------------|---------|
| 1     | 1                      | 3                    | 1                                   | 396.00                | 15                 | 58.66   |
| 2     | 1                      | 3                    | 1                                   | 396.00                | 30                 | 68.90   |
| 3     | 1                      | 3                    | 1                                   | 396.00                | 60                 | 67.38   |
| 4     | 1                      | 3                    | 1                                   | 396.00                | 120                | 73.56   |
| 5     | 1                      | 3                    | 2                                   | 198.00                | 15                 | 82.69   |
| 6     | 1                      | 3                    | 2                                   | 198.00                | 30                 | 81.77   |
| 7     | 1                      | 3                    | 2                                   | 198.00                | 60                 | 84.00   |
| 8     | 1                      | 3                    | 2                                   | 198.00                | 120                | 81.31   |
| 9     | 2                      | 3                    | 2                                   | 264.00                | 15                 | 83.35   |
| 10    | 2                      | 3                    | 2                                   | 264.00                | 30                 | 81.34   |
| 11    | 2                      | 3                    | 2                                   | 264.00                | 60                 | 84.36   |
| 12    | 2                      | 3                    | 2                                   | 264.00                | 120                | 84.81   |
| 13    | 2                      | 3                    | 2.5                                 | 211.00                | 15                 | 86.50   |
| 14    | 2                      | 3                    | 2.5                                 | 211.00                | 30                 | 83.42   |
| 15    | 2                      | 3                    | 2.5                                 | 211.00                | 60                 | 86.03   |
| 16    | 2                      | 3                    | 2.5                                 | 211.00                | 120                | 83.96   |

|    |      |   |     |         |      |       |
|----|------|---|-----|---------|------|-------|
| 17 | 5    | 3 | 3   | 220.00  | 15   | 26.43 |
| 18 | 5    | 3 | 3   | 220.00  | 30   | 23.54 |
| 19 | 5    | 3 | 3   | 220.00  | 60   | 26.56 |
| 20 | 5    | 3 | 3   | 220.00  | 120  | 22.69 |
| 21 | 2    | 3 | 3   | 176.00  | 15   | 85.89 |
| 22 | 2    | 3 | 3   | 176.00  | 30   | 85.06 |
| 23 | 2    | 3 | 3   | 176.00  | 60   | 86.15 |
| 24 | 2    | 3 | 3   | 176.00  | 120  | 86.60 |
| 25 | 1    | 1 | N/A | 1050.00 | 15   | 22.78 |
| 26 | 1    | 1 | N/A | 1050.00 | 30   | 20.73 |
| 27 | 1    | 1 | N/A | 1050.00 | 60   | 25.78 |
| 28 | 1    | 1 | N/A | 1050.00 | 120  | 34.79 |
| 29 | 0.25 | 1 | N/A | 53.00   | 15   | 25.45 |
| 30 | 0.67 | 1 | N/A | 105.00  | 15   | 21.68 |
| 31 | 1.5  | 1 | N/A | 158.00  | 15   | 43.06 |
| 32 | 4    | 1 | N/A | 210.00  | 15   | 33.07 |
| 33 | 1    | 1 | N/A | 132.00  | 2    | 15.16 |
| 34 | 1    | 1 | N/A | 132.00  | 5    | 17.39 |
| 35 | 1    | 1 | N/A | 132.00  | 15   | 66.80 |
| 36 | 1    | 1 | N/A | 132.00  | 30   | 66.57 |
| 37 | 1    | 1 | N/A | 132.00  | 60   | 66.03 |
| 38 | 1    | 1 | N/A | 132.00  | 120  | 60.62 |
| 39 | 1    | 3 | 1   | 396.00  | 2880 | 84.59 |
| 40 | 1    | 1 | N/A | 818.00  | 15   | 69.91 |
| 41 | 1    | 1 | N/A | 818.00  | 30   | 74.83 |
| 42 | 1    | 1 | N/A | 818.00  | 60   | 72.07 |
| 43 | 1    | 1 | N/A | 818.00  | 90   | 77.65 |
| 44 | 1    | 1 | N/A | 818.00  | 120  | 62.82 |
| 45 | 2    | 3 | 3   | 176.00  | 1    | 13.38 |
| 46 | 2    | 3 | 3   | 176.00  | 2    | 53.50 |
| 47 | 2    | 3 | 3   | 176.00  | 3    | 69.82 |
| 48 | 2    | 3 | 3   | 176.00  | 5    | 81.92 |
| 49 | 2    | 3 | 3   | 176.00  | 15   | 81.38 |
| 50 | 1    | 3 | 3   | 132.53  | 15   | 82.7  |
| 51 | 3    | 3 | 3   | 198.11  | 15   | 47.38 |
| 52 | 4    | 3 | 3   | 35.34   | 15   | 23.06 |
| 53 | 0.67 | 3 | 3   | 17.67   | 15   | 21.7  |
| 54 | 0.25 | 3 | 3   | 8.83    | 15   | 25.45 |
| 55 | 2    | 3 | 1   | 528.30  | 15   | 68.8  |
| 56 | 5    | 3 | 1   | 660.40  | 15   | 20.7  |

|    |      |   |   |        |     |       |
|----|------|---|---|--------|-----|-------|
| 57 | 3    | 3 | 1 | 594.35 | 15  | 42.5  |
| 58 | 3    | 3 | 2 | 297.17 | 15  | 51.6  |
| 59 | 0.25 | 3 | 2 | 79.24  | 15  | 22.9  |
| 60 | 4    | 3 | 3 | 35.34  | 30  | 25.87 |
| 61 | 4    | 3 | 3 | 35.34  | 60  | 41.33 |
| 62 | 4    | 3 | 3 | 35.34  | 120 | 44.60 |
| 63 | 0.25 | 3 | 3 | 8.83   | 30  | 24.53 |
| 64 | 0.25 | 3 | 3 | 8.83   | 60  | 22.90 |
| 65 | 0.25 | 3 | 3 | 8.83   | 120 | 24.30 |
| 66 | 0.25 | 3 | 3 | 8.83   | 90  | 24.21 |
| 67 | 0.67 | 3 | 3 | 17.67  | 60  | 27.60 |
| 68 | 0.67 | 3 | 3 | 17.67  | 120 | 28.40 |
| 69 | 3    | 3 | 3 | 198.11 | 15  | 47.38 |
| 70 | 3    | 3 | 3 | 198.11 | 30  | 56.43 |
| 71 | 3    | 3 | 3 | 198.11 | 60  | 59.70 |
| 72 | 3    | 3 | 3 | 198.11 | 120 | 58.20 |
| 73 | 1    | 3 | 3 | 132.53 | 90  | 85.21 |
| 74 | 2    | 3 | 3 | 176.00 | 90  | 87.93 |
| 75 | 3    | 3 | 3 | 198.11 | 90  | 55.19 |
| 76 | 4    | 3 | 3 | 35.34  | 90  | 42.03 |
| 77 | 5    | 3 | 3 | 220.00 | 90  | 28.13 |

**Table S4.** Yields are calculated based on the conversion of Zr metal to MOF-808. Chemical formula for MOF-808 ( $\text{Zr}_6\text{O}_4(\text{OH})_4(\text{BTC})_2(\text{HCOO})_6$ ) has a molecular weight of 1363.8 g/mol.  $\text{H}_3\text{BTC}$  linker has a molecular weight of 210.14 g/mol. About 64.67 mg (0.2 mmol) of Zr salt was used in the precursor mixture. Below is an example calculation for yield in case of a flow synthesized sample, Run #21 in Table S3. The procedure has been adapted from Garzon-Tovar et al.<sup>26</sup> and Furukawa et al.<sup>27</sup>

$$\text{Yield (\%)} = \left( \frac{\text{Activated Solids Obtained from Synthesis}}{\text{Solids Obtained from 100\% Zr Conversion}} \right) \times 100 \quad (\text{Equation S10})$$

| Compound                                   | Molar Mass | Solids Obtained for 100% Conversion of $\text{ZrOCl}_2 \cdot 8\text{H}_2\text{O}$ to MOF-808 | Solids Obtained (non-activated) | Mass of Activated Solids | Yield |
|--|------------|--|---------------------------------|--------------------------|-------|
|  | g/mol      | g  | g                               | g                        | %     |
| $\text{ZrOCl}_2 \cdot 8\text{H}_2\text{O}$ | 322.25     | 0.0912   | 0.085                           | 0.073                    | 80.12 |

**Table S5.** Calculation of process productivity ( $kg_{MOF} m^{-3} day^{-1}$ ) for batch and flow syntheses of MOF-808 is shown in the table below. Productivity is defined as kg of solids synthesized, per  $m^3$  of precursor mixture per day. Solids obtained for 1 and 3 min are amorphous and semi-crystalline.

$$Productivity (kg m^{-3} day^{-1}) = \frac{\text{Production Rate } \left(\frac{kg}{day}\right)}{\text{Precursor Feed Rate } \left(\frac{m^3}{h}\right) \times 24h} \quad (\text{Equation S11})$$

| Synthesis Route       | Res. Time (min) | Non-Activated Solids Obtained ( $mg mL^{-1}$ ) | Precursor Consumed ( $mL day^{-1}$ ) | Productivity               | Yield (%) |
|-----------------------|-----------------|--|--------------------------------------|----------------------------|-----------|
|                       |                 |  |                                      | $kg_{MOF} m^{-3} day^{-1}$ |           |
| <b>Flow @ 150 °C</b>  | 1               | 17.7   | 16128                                | 285465.6                   | ~ 55      |
|                       | 3               | 29.5   | 5112                                 | 150804                     | ~ 80      |
|                       | 5               | 29.5   | 3225.6                               | 95155.2                    | ~ 80      |
|                       | 15              | 29.5   | 1075.6                               | 31730.2                    | ~ 80      |
|                       | 30              | 29.5   | 538.5                                | 15887.5                    | ~ 80      |
|                       | 60              | 29.5   | 269.2                                | 7943.7                     | ~ 80      |
|                       | 120             | 29.5   | 135.3                                | 3993.1                     | ~ 80      |
| <b>Batch @ 130 °C</b> | 2880            | 0.745  | 450                                  | 335.5                      | ~ 75      |

**Table S6.** Details of equipment used in batch and flow syntheses and calculation of operational cost of equipment (in \$/day).

| Process      | Equipment Description                 | Units | Purchase Price | Maintenance & Consumables | Equipment Life-time | Total \$ | \$/day          |
|--------------|---------------------------------------|-------|----------------|---------------------------|---------------------|----------|-----------------|
|              |                                       | #     | \$             | \$                        | days                |          |                 |
| <b>Batch</b> | Magnetic Stirrer                      | 2     | 93.90          | 112.68                    | 1825.00             | 225.36   | 0.12            |
|              | Ultrasonication                       | 1     | 400.00         | 480.00                    | 2190.00             | 480.00   | 0.22            |
|              | Convection Oven                       | 1     | 4500.00        | 5400.00                   | 2190.00             | 5400.00  | 2.47            |
|              | Pyrex Glass Jars                      | 4     | 250.00         | 300.00                    | 2190.00             | 1200.00  | 0.55            |
|              | Centrifuge                            | 1     | 35000.00       | 42000.00                  | 2555.00             | 42000.00 | 16.44           |
|              | Vacuum/Drying Oven                    | 1     | 7500.00        | 9000.00                   | 2555.00             | 9000.00  | 3.52            |
|              | Sample Storage, Consumables           | 1     | 600.00         | 720.00                    | 1825.00             | 720.00   | 0.39            |
|              | <b>Total Cost</b>                     |       |                |                           |                     |          | <b>59025.36</b> |
| <b>Flow</b>  | Magnetic Stirrer                      | 2     | 93.90          | 112.68                    | 1825.00             | 225.36   | 0.12            |
|              | Ultrasonication                       | 1     | 400.00         | 480.00                    | 2190.00             | 480.00   | 0.22            |
|              | Reactor                               | 1     | 400.00         | 480.00                    | 1825.00             | 480.00   | 0.26            |
|              | Syringe Pump                          | 1     | 4000.00        | 4800.00                   | 3650.00             | 4800.00  | 1.32            |
|              | SS Syringes                           | 2     | 800.00         | 960.00                    | 2920.00             | 1920.00  | 0.66            |
|              | Oil Pump                              | 1     | 3000.00        | 3600.00                   | 2920.00             | 3600.00  | 1.23            |
|              | Laptop                                | 1     | 400.00         | 480.00                    | 2190.00             | 480.00   | 0.22            |
|              | Temp Control                          | 1     | 200.00         | 240.00                    | 2190.00             | 240.00   | 0.11            |
|              | SS Sample Vials                       | 4     | 190.00         | 228.00                    | 1825.00             | 912.00   | 0.50            |
|              | Tube/Fittings                         | 1     | 1000.00        | 1200.00                   | 2190.00             | 1200.00  | 0.55            |
|              | Sample Storage and N <sub>2</sub> Gas | 1     | 900.00         | 1080.00                   | 2190.00             | 1080.00  | 0.49            |
|              | Centrifuge                            | 1     | 35000.00       | 42000.00                  | 2555.00             | 42000.00 | 16.44           |
|              | Vacuum/Drying Oven                    | 1     | 7500.00        | 9000.00                   | 2555.00             | 9000.00  | 3.52            |
|              | <b>Total Cost</b>                     |       |                |                           |                     |          | <b>66417.36</b> |

**Table S7.** Raw material costs for reagents used in the precursor mixture and solvents. Prices reflect the cheapest rates available for purchase from EMD Millipore Chemicals, Acros Organics, and Sigma-Aldrich. Bulk purchase price in case of commodity chemicals would be cheaper than the prices mentioned below.

| Reagent                              | Function      | Price Advertised |
|--------------------------------------|---------------|------------------|
|                                      |               | \$               |
| Zirconyl Chloride Octahydrate        | Zr Source     | \$626 / kg       |
| H <sub>3</sub> BTC (Trimesic Acid)   | Linker        | \$546 / kg       |
| <i>N,N</i> -dimethylformamide        | Solvent       | \$1662 / 50 L    |
| Formic Acid                          | Modulator     | \$755 / 10 L     |
| Silicone Oil (Flow Synthesis)        | Carrier Fluid | \$66.7 / L       |
| Acetone                              | Solvent       | \$20.16 / L      |
| <i>N,N</i> -dimethylformamide (Bulk) | Solvent       | \$1.41 / L       |
| Formic Acid (Bulk)                   | Modulator     | \$1.58 / L       |

**Table S8.** Energy accounting for each unit operation to synthesize MOF-808 in batch and flow process. Crystallization step is different for both processes, while rest of the operations remain the same.

| Unit Operation                             | Process Equipment              | Power Rating | Time Used | Energy Consumed | Electricity Cost | Total Cost    |
|--|--------------------------------|--------------|-----------|-----------------|------------------|---------------|
|  |                                | W            | h         | kWh             | \$/kWh           | \$            |
| <b>Precursor Mixing</b>                    | Magnetic Stirrer               | 4            | 0.5000    | 0.0018          | <b>0.120</b>     | 0.0002        |
| <b>Crystallization (Batch) *</b>           | Forced Convection Oven         | 1200         | 48.166    | 57.800          |                  | 6.9360        |
| <b>Crystallization (Flow) *</b>            | Sleeve Heater                  | 200          | 0.6418    | 0.1284          |                  | 0.0154        |
|  | Pump (Oil)                     | 10           | 0.2833    | 0.0028          |                  | 0.0003        |
|  | Syringe Pump                   | 35           | 0.1166    | 0.0041          |                  | 0.0005        |
|  | Mag. Stirrer - Syringe         | 4            | 0.1166    | 0.0004          |                  | 0.0001        |
|  | Temp. Controller               | 40           | 0.6418    | 0.0257          |                  | 0.0003        |
|  | Computer                       | 50           | 0.6418    | 0.0321          |                  | 0.0039        |
| <b>Centrifuge</b>                          | Product Separation             | 800          | 0.2000    | 0.1600          |                  | 0.0192        |
| <b>Vacuum Drying Oven</b>                  | Solvent Removal and Activation | 3500         | 0.0833    | 0.2916          |                  | 0.0350        |
| <b>\$ Cost of Energy (Batch Synthesis)</b> |                                |              |           |                 |                  | <b>6.9904</b> |
| <b>\$ Cost of Energy (Flow Synthesis)</b>  |                                |              |           |                 |                  | <b>0.0776</b> |

\* Time used for Scenario 2 (continuous production) would be 24 h instead of the values mentioned in the table above.

**Table S9.** Definitions of parameters used in the techno-economic analysis.

| <b>Parameter</b>    | <b>Unit</b>          | <b>Definition</b>   |
|---------------------|----------------------|---|
| $C_{materials}$     | \$                   | Total cost of materials (in all unit operations) involved in MOF synthesis.               |
| $C_{energy}$        | \$                   | Total cost of energy (in all unit operations) involved in MOF synthesis.                  |
| $C_{equipment}$     | \$                   | Total cost of equipment (in all unit operations) involved in MOF synthesis.               |
| $n_{machine}$       | #                    | Number of identical machines used for the production process.                             |
| $C_{machine}$       | \$                   | Cost of a specific machine used in the production process.                                |
| $C_{Mnt. \& Cons.}$ | \$                   | Cost of maintenance and consumables for a specific machine.                               |
| $t_{life-time}$     | days                 | Lifetime for a machine.   |
| $E_{machine}$       | kWh                  | Energy consumed by the machine (Power Rating * Usage Time).                               |
| $C_{electricity}$   | \$.kWh <sup>-1</sup> | Unit cost of electricity.   |
| $C_{Zr}$            | \$                   | Cost of Zr metal salt (ZrOCl <sub>2</sub> .8H <sub>2</sub> O) used in synthesis.          |
| $C_{linker}$        | \$                   | Cost of H <sub>3</sub> BTC linker used in synthesis.                                      |
| $C_{modulator}$     | \$                   | Cost of formic acid modulator used in synthesis.  |
| $C_{solvents}$      | \$                   | Cost of DMF and Acetone used in synthesis and post-process.                               |
| $E_{process}$       | kWh.g <sup>-1</sup>  | Energy intensity (or consumption) of the process, normalized to per g of MOF synthesized. |

|                 |   |  |
|-----------------|---|--|
| $GHG_{grid}$    | kgCO <sub>2</sub> -eq<br>.kWh <sup>-1</sup> | GHG (Greenhouse Gas) emissions per kWh generation for ISO-NE grid. |
| $C_{operation}$ | \$.day <sup>-1</sup>                        | Operational cost of equipment amortized over its useful lifetime.  |
| $P_{MOF-808}$   | g.day <sup>-1</sup>                         | Production rate of MOF-808   |

**Table S10.** Thermal properties of reaction mixture used in Batch and Flow synthesis.

| Synthesis Route   | Density of Rxn Mixture (g mL <sup>-1</sup> ) | Mass of Rxn Mixture (kg) | Specific Heat Capacity $c$ (J kg <sup>-1</sup> K <sup>-1</sup> ) | Reaction Conditions | $Q = mc\Delta T$ (kJ) |
|-------------------|--|--------------------------|--|---------------------|-----------------------|
| Batch (Precursor) | 0.967  | 0.1301                   | 1488.99  | 130 °C, 48 h        | 22.27                 |
| Flow (Precursor)  | 0.956  | 0.0318                   | 1372.16  | 150 °C, 15 min      | 5.68                  |
| Flow (Oil)        | 0.963  | 0.0161                   | 2000.00  | 150 °C, 15 min      | 4.17                  |

**Table S11.** Comparison of defects generated in flow and batch synthesized MOF-808.

Shorter reaction times and faster growth kinetics in flow synthesized samples could be attributed to higher percent of missing-linker defect concentration in samples prepared in flow compared to batch. Defect content was calculated from the ratio of  $N_d$  (actual number of linkers per Zr<sub>6</sub> node) to  $N_t$  (theoretical number of linkers per Zr<sub>6</sub> node). For example, considering that 100 g (0.816 mol) of ZrO<sub>2</sub> originates from 0.135 mol of Zr<sub>6</sub> clusters, the corresponding mass of the Zr<sub>6</sub> cluster would

be 91.86 g. Thus, the remaining mass leftover ( $k$ ) after combustion in the TGA (at 600 °C) would originate from the H<sub>3</sub>BTC linker and  $k$  accounts for mass difference between ZrO<sub>2</sub> and Zr<sub>6</sub> cluster. The amount of linker detected on each Zr<sub>6</sub> node is measured by  $A_d$  in mol. The theoretical amount of linker per Zr<sub>6</sub> node ( $A_t$ ) corresponds to 0.271 mol for H<sub>3</sub>BTC.

$$A_d = \left( \frac{TGA-Residual\ ZrO_2+k}{M_w} \right) \quad (\text{Equation S12})$$

$$N_d = \left( \frac{A_d \times N_t}{A_t} \right) \times 100 \quad (\text{Equation S13})$$

$$Defects\ (\%) = \left( 1 - \frac{N_d}{N_t} \right) \times 100 \quad (\text{Equation S14})$$

|              | <b>Residence Time</b> | <b>% Defects</b> | <b>N<sub>t</sub></b> | <b>N<sub>d</sub></b> |
|--------------|-----------------------|------------------|----------------------|----------------------|
| <b>Flow</b>  | 3 min                 | 9.505            | 2                    | 1.809                |
|              | 5 min                 | 12.534           | 2                    | 1.749                |
|              | 15 min                | 20.568           | 2                    | 1.588                |
|              | 30 min                | 17.178           | 2                    | 1.656                |
|              | 60 min                | 15.572           | 2                    | 1.688                |
|              | 120 min               | 15.037           | 2                    | 1.699                |
| <b>Batch</b> | 48 hours              | 4.01             | 2                    | 1.919                |

**Table S12.** Comparison of pore volumes for samples with RC values greater than 80%. All samples had a RLC=3 and FA:DMF=2.

| <b>Residence Time</b> | <b>RC</b> | <b>BET Surface Area (m<sup>2</sup>/g)</b> | <b>Pore Volume (cm<sup>3</sup>/g)</b> |
|-----------------------|-----------|---|---------------------------------------|
| <b>5 min</b>          | 81.9 %    | 1585                                      | 1.025                                 |
| <b>15 min</b>         | 85.9 %    | 1980                                      | 1.645                                 |
| <b>30 min</b>         | 85.1 %    | 1936                                      | 1.610                                 |
| <b>60 min</b>         | 86.2 %    | 1969                                      | 1.487                                 |
| <b>120 min</b>        | 86.6 %    | 1824                                      | 1.130                                 |

## References:

1. Bagi, S.; Wright, A. M.; Oppenheim, J.; Dincă, M.; Román-Leshkov, Y., Accelerated Synthesis of a Ni<sub>2</sub>Cl<sub>2</sub>(BTDD) Metal–Organic Framework in a Continuous Flow Reactor for Atmospheric Water Capture. *Acs Sustain Chem Eng* **2021**, *9* (11), 3996-4003. doi:10.1021/acssuschemeng.0c07055.
2. Bagi, S. D.; Myerson, A. S.; Román-Leshkov, Y., Solvothermal Crystallization Kinetics and Control of Crystal Size Distribution of MOF-808 in a Continuous Flow Reactor. *Crystal Growth & Design* **2021**, *21* (11). doi:10.1021/acs.cgd.1c00968.
3. Jiang, J.; Gándara, F.; Zhang, Y.-B.; Na, K.; Yaghi, O. M.; Klemperer, W. G., Superacidity in Sulfated Metal–Organic Framework-808. *J Am Chem Soc* **2014**, *136* (37), 12844-12847. doi:10.1021/ja507119n.
4. Sonneveld, E. J.; Visser, J. W., Automatic Collection of Powder Data from Photographs. *J Appl Crystallogr* **1975**, *8* (Feb1), 1-7. doi:10.1107/S0021889875009417.
5. Hirschle, P.; Preiß, T.; Auras, F.; Pick, A.; Völkner, J.; Valdepérez, D.; Witte, G.; Parak, W. J.; Rädler, J. O.; Wuttke, S., Exploration of MOF nanoparticle sizes using various physical characterization methods – is what you measure what you get? *CrystEngComm*. **2016**, *18* (23), 4359-4368. doi:10.1039/c6ce00198j.
6. Gómez-Gualdrón, D. A.; Moghadam, P. Z.; Hupp, J. T.; Farha, O. K.; Snurr, R. Q., Application of Consistency Criteria To Calculate BET Areas of Micro- And Mesoporous Metal–Organic Frameworks. *J Am Chem Soc* **2015**, *138* (1), 215-224. doi:10.1021/jacs.5b10266.
7. Jia, C. M.; Cirujano, F. G.; Bueken, B.; Claes, B.; Jonckheere, D.; Van Geem, K. M.; De Vos, D., Geminal Coordinatively Unsaturated Sites on MOF-808 for the Selective Uptake of Phenolics from a Real Bio-Oil Mixture. *Chemsuschem* **2019**, *12* (6), 1256-1266. doi:10.1002/cssc.201802692.
8. Vermoortele, F.; Bueken, B.; Le Bars, G.; Van de Voorde, B.; Vandichel, M.; Houthoofd, K.; Vimont, A.; Daturi, M.; Waroquier, M.; Van Speybroeck, V.; Kirschhock, C.; De Vos, D. E., Synthesis Modulation as a Tool To Increase the Catalytic Activity of Metal–Organic Frameworks: The Unique Case of UiO-66(Zr). *J Am Chem Soc* **2013**, *135* (31), 11465-11468. doi:10.1021/ja405078u.
9. Smart, C.; Reese, G.; Adams, L.; Batchelor, A.; Redrick, A., Process-Based Cost Modeling. *Journal of Parametrics* **2011**, *26* (1), 79-100. doi:10.1080/10157891.2007.10462279.
10. DeSantis, D.; Mason, J. A.; James, B. D.; Houchins, C.; Long, J. R.; Veenstra, M., Techno-economic Analysis of Metal–Organic Frameworks for Hydrogen and Natural Gas Storage. *Energy & Fuels* **2017**, *31* (2), 2024-2032. doi:10.1021/acs.energyfuels.6b02510.
11. Jimenez-Gonzalez, C. n.; Curzons, A. D.; Constable, D. J. C.; Cunningham, V. L., Expanding GSK's Solvent Selection Guide? application of life cycle assessment to enhance solvent selections. *Clean Technologies and Environmental Policy* **2004**, *7* (1), 42-50. doi:10.1007/s10098-004-0245-z.
12. Kalinovskyy, Y.; Cooper, N. J.; Main, M. J.; Holder, S. J.; Blight, B. A., Microwave-assisted activation and modulator removal in zirconium MOFs for buffer-free CWA hydrolysis. *Dalton T* **2017**, *46* (45), 15704-15709. doi:10.1039/c7dt03616g.
13. Liang, W.; Chevreau, H.; Ragon, F.; Southon, P. D.; Peterson, V. K.; D'Alessandro, D. M., Tuning pore size in a zirconium–tricarboxylate metal–organic framework. *CrystEngComm* **2014**, *16* (29), 6530-6533. doi:10.1039/c4ce01031k.

14. Reinsch, H.; Waitschat, S.; Chavan, S. M.; Lillerud, K. P.; Stock, N., A Facile “Green” Route for Scalable Batch Production and Continuous Synthesis of Zirconium MOFs. *Eur J Inorg Chem* **2016**, *2016* (27), 4490-4498. doi:10.1002/ejic.201600295.
15. Torlakovic, G.; Torlakovic, E.; Skovlund, E.; Nesland, J. M.; Reith, A.; Danielsen, H. E., Volume-related sequence of tumor distribution pattern in prostate carcinoma: Importance of posterior midline crossover in predicting tumor volume, extracapsular extension, and seminal vesicle invasion. *Croat Med J* **2005**, *46* (3), 429-435.
16. Fitzpatrick, D. E.; Ley, S. V., Engineering chemistry: integrating batch and flow reactions on a single, automated reactor platform. *React Chem Eng* **2016**, *1* (6), 629-635. doi:10.1039/c6re00160b.
17. Liu, Z. D.; Zhu, J.; Wakihara, T.; Okubo, T., Ultrafast synthesis of zeolites: breakthrough, progress and perspective. *Inorg Chem Front* **2019**, *6* (1), 14-31. doi:10.1039/c8qi00939b.
18. Rubio-Martinez, M.; Avci-Camur, C.; Thornton, A. W.; Imaz, I.; Maspocho, D.; Hill, M. R., New synthetic routes towards MOF production at scale. *Chem Soc Rev* **2017**, *46* (11), 3453-3480. doi:10.1039/c7cs00109f.
19. Dunne, P. W.; Lester, E.; Walton, R. I., Towards scalable and controlled synthesis of metal-organic framework materials using continuous flow reactors. *React Chem Eng* **2016**, *1* (4), 352-360. doi:10.1039/c6re00107f.
20. Kockmann, N.; Roberge, D. M., Harsh Reaction Conditions in Continuous-Flow Microreactors for Pharmaceutical Production. *Chem Eng Technol* **2009**, *32* (11), 1682-1694. doi:10.1002/ceat.200900355.
21. Smith, K. J.; Carter, P. S.; Bridges, A.; Horrocks, P.; Lewis, C.; Pettman, G.; Clarke, A.; Brown, M.; Hughes, J.; Wilkinson, M.; Bax, B.; Reith, A., The structure of MSK1 reveals a novel autoinhibitory conformation for a dual kinase protein. *Structure* **2004**, *12* (6), 1067-1077. doi:10.1016/j.str.2004.02.040.
22. Sudbo, J.; Samuelsson, R.; Risberg, B.; Heistein, S.; Nyhus, C.; Samuelsson, M.; Puntervold, R.; Sigstad, E.; Davidson, B.; Reith, A.; Berner, A., Risk markers of oral cancer in clinically normal mucosa as an aid in smoking cessation counseling (Retracted Article. See vol 24, pg 5621, 2006). *J Clin Oncol* **2005**, *23* (9), 1927-1933. doi:10.1200/Jco.2005.03.172.
23. Chaudhuri, J. P.; Kasprzycki, E.; Battaglia, M.; McGill, J. R.; Brogger, A.; Walther, J. U.; Reith, A., Biphasic chromatin structure and FISH signals reflect intranuclear order. *Cell Oncol* **2005**, *27* (5-6), 327-334.
24. Rubio-Martinez, M.; Hadley, T. D.; Batten, M. P.; Constanti-Carey, K.; Barton, T.; Marley, D.; Monch, A.; Lim, K. S.; Hill, M. R., Scalability of Continuous Flow Production of Metal-Organic Frameworks. *Chemsuschem* **2016**, *9* (9), 938-941. doi:10.1002/cssc.201501684.
25. Zhang, J.; Wang, K.; Teixeira, A. R.; Jensen, K. F.; Luo, G., Design and Scaling Up of Microchemical Systems: A Review. *Annual Review of Chemical and Biomolecular Engineering* **2017**, *8* (1), 285-305. doi:10.1146/annurev-chembioeng-060816-101443.
26. Garzon-Tovar, L.; Cano-Sarabia, M.; Carne-Sanchez, A.; Carbonell, C.; Imaz, I.; Maspocho, D., A spray-drying continuous-flow method for simultaneous synthesis and shaping of microspherical high nuclearity MOF beads. *React Chem Eng* **2016**, *1* (5), 533-539. doi:10.1039/c6re00065g.
27. Furukawa, H.; Gandara, F.; Zhang, Y. B.; Jiang, J. C.; Queen, W. L.; Hudson, M. R.; Yaghi, O. M., Water Adsorption in Porous Metal-Organic Frameworks and Related Materials. *J Am Chem Soc* **2014**, *136* (11), 4369-4381. doi:10.1021/ja500330a.